Hindawi Publishing Corporation
Mathematical Problems in Engineering
Volume 2016, Article ID 3698525, 10 pages
http://dx.doi.org/10.1155/2016/3698525

*Research Article*

# A Numerical Approach for the Quasi-Plane Strain-Softening Problem of Cylindrical Cavity Expansion Based on the Hoek-Brown Failure Criterion

**Jin-feng Zou and Jia-min Du**

*School of Civil Engineering, Central South University, No. 22, Shaoshan South Road, Central South University Railway Campus, Changsha, Hunan Province 410075, China*

Correspondence should be addressed to Jin-feng Zou; zoujinfeng_csu@163.com

Received 12 April 2016; Revised 26 June 2016; Accepted 20 July 2016

Academic Editor: Sebastian Heidenreich



This paper focuses on a novel approach for the quasi-plane strain-softening problem of the cylindrical cavity expansion based on generalized Hoek-Brown failure criterion. Because the intermediate principal stress is deformation-dependent, the quasi-plane strain problem is defined to implement the numerical solution of the intermediate principal stress. This approach assumes that the initial total strain in axial direction is a nonzero constant ($\varepsilon_0$) and the plastic strain in axial direction is not zero. Based on 3D failure criterion, the numerical solution of plastic strain is given. Solution of the intermediate principal stress can be derived by Hooke's law. The radial and circumferential stress and strain considering the intermediate principal stress are obtained by the proposed approach of the intermediate principal stress, stress equilibrium equation, and generalized H-B failure criterion. The numerical results can be used for the solution of strain-softening surrounding rock. In additional, the validity and accuracy of the proposed approach are verified with the published results. At last, parametric studies are carried out using MATLAB programming to highlight the influences of the out-of-plane stress on the stress and displacement of surrounding rock.

## 1. Introduction

Cavity expansion theory has been widely used in Geotechnical Engineering such as pressuremeter test and other geotechnical problems. Based on the Mohr-Coulomb (M-C) and Hoek-Brown (H-B) failure criteria, many researchers have solved many engineering problems using the analytical solution and semianalytical solution. Vesic [1] proposed an approximate solution based on the Mohr-Coulomb failure criterion for both spherical and cylindrical cavity expansion problems. Carter et al. [2] presented an explicit pressure-expansion relation and derived an analytical solution for cavity expansion in nonassociated Mohr-Coulomb media. Durban and Papanastasiou [3], enhanced the solutions of cylindrical cavity expansion and contraction in pressure sensitive geomaterials for the Tresca and Mises models, by incorporating pressure sensitivity in the plastic potential and effective stress. Durban [4–6] proposed the large strain and general solutions for pressurized elastoplastic tubes, and the finite straining of pressurized compressible elastoplastic tubes, respectively. Papanastasiou and Durban presented the elastoplastic analysis method of cylindrical cavity problems in geomaterials. Papanastasiou discussed the influence of plasticity in hydraulic fracturing. Collins and Yu [7] proposed the solutions for large strain undrained cavity expansion. Pan and Brown [8] considered the effects of out-of-plane stress and dilation on the convergence and stability of the surrounding rock. Cao et al. [9] expanded the solutions on modified Cam Clay model. Alonso et al. [10] obtained the self-similar solution for the circular tunnel in strain-softening rock masses. Lee and Pietruszczak [11] and Park et al. [12] presented the solutions for the cavity expansion with unloading by finite difference method. Yang and Zou [13] presented a numerical solution of cavity expansion in the generalized H-B media. Chen and Abousleiman [14, 15] presented an analytical solution of cavity expansion based on the modified Cam-Clay model. Wang et al. [16] studied the influence of out-of-plane stress on the distribution of stress, strain, and displacement based on plane strain assumption. Zhou et al. [17–19] proposed an analytical solution considering the influence of the shear stress on cylindrical cavity expansion in an undrained elastic-perfect soil.

Although some literatures [8, 16–22] focused on the effect of out-of-plane stress have been published, those studies assume that the plastic strain in axial direction is zero and the plastic potential function is simple. For example, Pan and Brown [8] proposed an approach in which the axial in situ stress of the plastic zone is deformation-dependent and the formula for the calculation of intermediate principal stress was derived, only numerical solution through finite element method was presented.

In the presented solutions, a numerical stepwise procedure that considers the quasi-plane strain-softening behavior is adopted and improved, where the deterioration of strength, deformation, and dilation angle in the plastic region are considered. The improved constitutive model considers the strain-softening behavior and the deformation dependence of intermediate principal stress compatible with generalized H-B failure criterion.

## 2. Objective and Scope

The main objective of the present study is to introduce a novel approach for the mechanical analysis of cylindrical cavity expansion considering the influence of the axial stress based on the assumptions of the quasi-plane strain-softening problem, and the corresponding theoretical solutions for the deformation-dependent intermediate principal stress and axial strain are proposed.

## 3. Methodology

*3.1. Definition of the Problem and Assumptions.* As shown in Figure 1, a cylindrical cavity expansion with an initial radius ($a_0$) is subjected to a hydrostatic pressure ($p_0$) in rock mass which is considered as continuous, homogeneous, isotropic, and initially elastic. The out-of-plane stress ($\sigma_z$) along the axis direction of the cylindrical cavity is also considered. The cylindrical cavity expands to a radius of $a$ as the internal cavity pressure increases from $p$ to $p_i$. Correspondingly, an element initially located at a distance ($r_0$) from the centre of the cavity wall moves to a new radial position ($r$). The region of rock mass around the cylindrical cavity is in the elastic state when the cylindrical cavity expansion pressure $p$ is small. As the cylindrical cavity expansion pressure $p$ increases to the critical value, the plastic region of rock mass around the cavity would appear with plastic deformation. If the cylindrical cavity expansion pressure $p$ increases continually, the plastic flow zone is formed, and the strength of surrounding rock mass around cavity is reduced to the residual strength. The cylindrical cavity expands to a radius of $a$ as the internal cavity pressure increases from $p$ to $p_i$. The plastic region around the cylindrical cavity is divided into two areas (i.e., plastic strain-softening region ($r_p$) and plastic flowing region ($r_s$)). The rock mass beyond the plastic region would remain elastic.

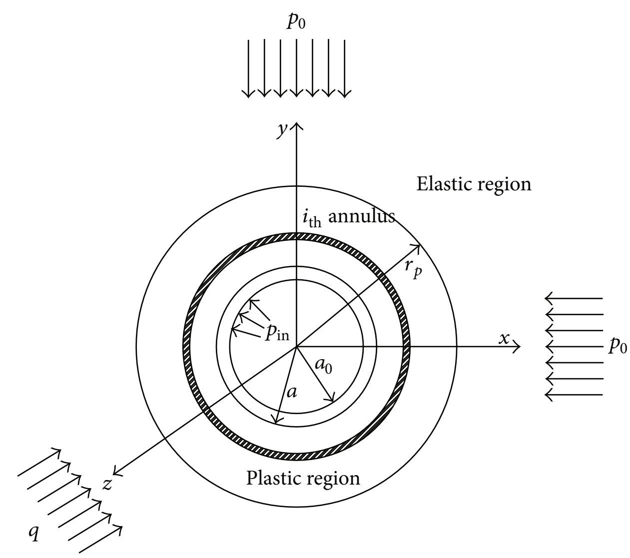


FIGURE 1: Model of the axisymmetric and quasi-plane strain-softening problem for cylindrical cavity expansion.

*3.2. Hoek-Brown Failure Criterion.* The generalized Hoek-Brown failure criterion is adopted and expressed by [22–24]

$$\sigma_1 = \sigma_3 + \sigma_c \left( \frac{m\sigma_3}{\sigma_c} + s \right)^a, \tag{1}$$

where $\sigma_1$ and $\sigma_3$ are the major and minor principal stresses, respectively. $\sigma_c$ is the uniaxial compressive strength of the rock mass. $a$, $m$, and $s$ are the strength parameters of the generalized H-B failure criterion. These variables are expressed as $m = m_i \exp[(\text{GSI} - 100)/(28 - 14D)]$, $s = \exp[(\text{GSI} - 100)/(9 - 3D)]$, and $n = 1/2 + [\exp(-\text{GSI}/15) - \exp(-20/3)]/6$. $D$ is a factor that depends on the degree of disturbance to which the rock has been subjected in terms of blast damage and stress relaxation. Its value varies between 0 and 1. GSI is the geological strength index of the rock mass, and its value ranges between 10 and 100.

*3.3. Plastic Potential Function.* In the paper, the plastic potential function based on 3D M-C failure criterion is adopted to obtain the solution of strain. The plastic potential function proposed by Pan and Brown [8] can be expressed by

$$Q(\sigma) = -\frac{n}{3} I_1 + \frac{3}{\sigma_c} J_2 + \frac{\sqrt{3}}{2} n \sqrt{J_2}, \tag{2}$$

where $I_1 = \sigma_1 + \sigma_2 + \sigma_3$, $J_2 = (1/6)[(\sigma_1 - \sigma_2)^2 + (\sigma_2 - \sigma_3)^2 + (\sigma_3 - \sigma_1)^2]$. $\sigma_1$, $\sigma_2$, and $\sigma_3$ are the major, intermediate, and minor principal stress, respectively. $n$ is the dilation parameter which is proposed by Pan and Brown [8].

Based on the plastic flow rule, the plastic strain increment is given by

$$d\varepsilon^p = \lambda \frac{\partial f}{\partial \sigma}. \tag{3}$$

The increments of major, intermediate, and minor plastic strains are presented by

$$\begin{aligned} d\varepsilon_1^p &= \left[\left(\frac{\sqrt{3}\left(2\sigma_1-\sigma_2-\sigma_3\right)}{12\sqrt{J_2}}-\frac{1}{3}\right)n \right.\\ &\quad \left. +\frac{1}{\sigma_c}\left(2\sigma_1-\sigma_2-\sigma_3\right)\right]d\lambda \\ d\varepsilon_2^p &= \left[\left(\frac{\sqrt{3}\left(2\sigma_2-\sigma_3-\sigma_1\right)}{12\sqrt{J_2}}-\frac{1}{3}\right)n \right.\\ &\quad \left. +\frac{1}{\sigma_c}\left(2\sigma_2-\sigma_3-\sigma_1\right)\right]d\lambda \\ d\varepsilon_3^p &= \left[\left(\frac{\sqrt{3}\left(2\sigma_3-\sigma_2-\sigma_1\right)}{12\sqrt{J_2}}-\frac{1}{3}\right)n \right.\\ &\quad \left. +\frac{1}{\sigma_c}\left(2\sigma_3-\sigma_2-\sigma_1\right)\right]d\lambda, \end{aligned} \tag{4}$$

where $\varepsilon_1^p$, $\varepsilon_2^p$, and $\varepsilon_3^p$ are the major, intermediate, and minor principal strains, respectively. $d\lambda$ is the plastic constant.

*3.4. Deterioration of Strength and Deformation Parameters of Surrounding Rock.* Based on the research results of Alonso et al. [10], the strength and deformation parameters of the strain-softening rock mass are evaluated based on plastic deformation and are controlled by the deviatoric strain

$$\gamma^p = \varepsilon_1^p - \varepsilon_3^p, \tag{5}$$

where $\varepsilon_1^p$ and $\varepsilon_3^p$ are the major and minor plastic strains, respectively.

The physical parameters of the surrounding rock mass are described according to the bilinear function of plastic shear strain as follows:

$$\omega\left(\gamma^p\right) = \begin{cases} \omega_p - \left(\omega_p - \omega_r\right)\dfrac{\gamma^p}{\gamma_r^p}, & 0 < \gamma^p < \gamma_r^p \\ \omega_r, & \gamma^p \geq \gamma_r^p, \end{cases} \tag{6}$$

where $\omega$ represents a strength parameter, such as $m$, $s$, and $a$; $\gamma_r^p$ is the critical deviatoric plastic strain from which the residual behavior is first observed and should be identified through experimentation. The subscripts $p$ and $r$ represent the peak and residual values, respectively.

When the axial force is considered as the middle principal stress, the elastic modulus and Poisson's ratio in the plastic zone of the deformation and stress evolution can be represented by a piecewise linear function as follows:

$$\begin{aligned} E\left(\gamma^p\right) &= \begin{cases} E_p - \left(E_p - E_r\right)\dfrac{\gamma^p}{\gamma_r^p}, & 0 < \gamma^p < \gamma_r^p \\ E_r, & \gamma^p \geq \gamma_r^p, \end{cases} \\ \nu\left(\gamma^p\right) &= \begin{cases} \nu_p - \left(\nu_p - \nu_r\right)\dfrac{\gamma^p}{\gamma_r^p}, & 0 < \gamma^p < \gamma_r^p \\ \nu_r, & \gamma^p \geq \gamma_r^p. \end{cases} \end{aligned} \tag{7}$$

To take into account the effect of variable dilation in the plastic region, dilation angle $\varphi(\gamma^p)$ presumably decreases linearly with strain from its peak value $\varphi_p$ at $\gamma_p = 0$ to the residual value $\varphi_r$ at $\gamma_p = \gamma_p^r$, as in the following equation:

$$\xi\left(\gamma^p\right) = \begin{cases} \xi_p - \left(\xi_p - \xi_r\right)\dfrac{\gamma^p}{\gamma_r^p}, & 0 < \gamma^p < \gamma_r^p \\ \xi_r, & \gamma^p \geq \gamma_r^p, \end{cases} \tag{8}$$

where $\xi_p$ and $\xi_r$ are the peak and residual values of the dilation angle of the rock, respectively; $\gamma^p$ is the softening parameter; $\gamma_r^p$ is the value of the softening parameter that controls the transition between the softening and residual stages. In (5)–(8), $\gamma^p$ is obtained by (5). $\gamma_r^p$ is the critical deviatoric plastic strain and should be determined through experimentation. The corresponding of parameters ($m$, $s$, and $a$) are as follows:

$$\begin{aligned} m\left(\gamma^p\right) &= \begin{cases} m_p - \left(m_p - m_r\right)\dfrac{\gamma^p}{\gamma_r^p}, & 0 < \gamma^p < \gamma_r^p \\ m_r, & \gamma^p \geq \gamma_r^p, \end{cases} \\ s\left(\gamma^p\right) &= \begin{cases} s_p - \left(s_p - s_r\right)\dfrac{\gamma^p}{\gamma_r^p}, & 0 < \gamma^p < \gamma_r^p \\ s_r, & \gamma^p \geq \gamma_r^p, \end{cases} \\ a\left(\gamma^p\right) &= \begin{cases} a_p - \left(a_p - a_r\right)\dfrac{\gamma^p}{\gamma_r^p}, & 0 < \gamma^p < \gamma_r^p \\ a_r, & \gamma^p \geq \gamma_r^p. \end{cases} \end{aligned} \tag{9}$$

$\xi_p$ and $\xi_r$ are the peak and residual values of the dilation angle of the rock and determined by experiments, respectively. Then, the deterioration parameters of strength and deformation of surrounding rock are determined [25].

## 4. Solutions of Stress and Displacement in Elastic Zone

*4.1. Equilibrium Equations and Stress Boundary Conditions.* Under the assumption of small deformation, the rock mass satisfies the generalized Hooke's law in the elastic region and obeys generalized H-B failure criterion in the plastic region. The stress equilibrium equation of an element near an cavity wall can be represented by

$$\frac{d\sigma_r}{dr} + \frac{\sigma_r - \sigma_\theta}{r} = 0, \tag{10}$$

where $\sigma_r$ is the radial stress; $\sigma_\theta$ is the tangential stress.

Stress boundary conditions can be given by

$$\begin{aligned} \sigma_r\big|_{r=r_0} &= p \\ \lim_{r\to\infty}\sigma_r &= \sigma_0. \end{aligned} \tag{11}$$

The relationship of the radial and the tangential stresses at the interface between the elastic and plastic zones is presented by

$$\sigma_\theta = 2\sigma_0 - \sigma_R. \tag{12}$$

The radial and the tangential stresses at the elastoplastic interface are satisfied with the yield criterion and can be given by

$$\sigma_R = \sigma_\theta + \sigma_c\left(\frac{m\sigma_\theta}{\sigma_c} + s\right)^a. \tag{13}$$

Combination of (12) and (13) leads to

$$\begin{Bmatrix}\sigma_r \\ \sigma_\theta \\ \sigma_z\end{Bmatrix} = \begin{Bmatrix}2\sigma_0 - \sigma_\theta \\ \sigma_\theta \\ q\end{Bmatrix}. \tag{14}$$

*4.2. Stress and Strain Solutions.* The solutions of stress and displacement in the elastic zone are expressed as follows [21, 22, 26]:

$$\begin{aligned}\sigma_r &= p_0 - (p_0 - \sigma_R)\left(\frac{R}{r}\right)^2 \\ \sigma_\theta &= p_0 + (p_0 - \sigma_R)\left(\frac{R}{r}\right)^2 \\ \sigma_z &= v(\sigma_\theta + \sigma_r) - 2vp_0 + q \\ u &= \frac{1}{2G}(\sigma_R - \sigma_0)\frac{R^2}{r},\end{aligned} \tag{15}$$

where $R$ is the plastic radius of surrounding rock, $v$ is Poisson's ratio, and $G = E/2(1+v)$ is the Shear modulus.

## 5. Stress and Strain in Plastic Region

Analytical solutions of stress and displacement are difficult to obtain in the strain-softening rock mass, especially considering the axial stress. In this paper, the quasi-plane strain and displacement of strain-softening rock mass are solved by iteration method which is illustrated by Figure 2.

The total plastic region is divided into $n$ connect annuli as shown in Figure 2. The $i$th annulus is delimitated by the internal radius with $\rho_{(j-1)} = r_{(j-1)}/R$ and the outer radius with $\rho_{(j)} = r_{(j)}/R$. The radius of the first ring is $\rho_{(0)} = 1$ which is at the interface between the elastic region and the plastic zone; the surrounding rock soil mass remains the critical state of the plastic.

The increment of radial stress results in the following:

$$\Delta\sigma_r = \frac{p_{\text{in}} - \sigma_R}{n}. \tag{16}$$

So the radial stress can be expressed by

$$\sigma_{r(i)} = \sigma_{r(i-1)} + \Delta\sigma_r. \tag{17}$$

The corresponding tangential stress is given by

$$\sigma_{r(i)} = \sigma_{\theta(i)} + \sigma_c\left(\frac{m_{(i-1)}\sigma_{\theta(i)}}{\sigma_c} + s_{(i-1)}\right)^{a_{(i-1)}}. \tag{18}$$

The axial stress $\sigma_{z(i)}$ proposed by Pan and Brown [8] can be represented by

$$\sigma_{z(i)} = \nu\left(\sigma_{r(i)} + \sigma_{\theta(i)}\right) + (1-2\nu)\sigma_0 - E\varepsilon^p_{z(i-1)}. \tag{19}$$

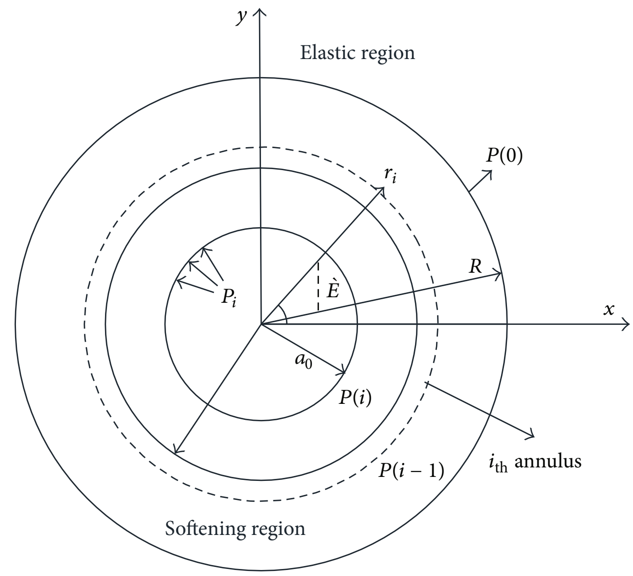


Figure 2: Normalized plastic region with finite number of annuli.

Combination of (17) and (18) leads to

$$\begin{aligned}\Delta\sigma_{\theta(i)} &= \sigma_{\theta(i)} - \sigma_{\theta(i-1)} \\ \Delta\sigma_{z(i)} &= \sigma_{z(i)} - \sigma_{z(i-1)}.\end{aligned} \tag{20}$$

The elastic strain can be expressed by

$$\begin{aligned}\varepsilon^e_r &= \frac{1}{E}\left[\sigma_r - \nu(\sigma_\theta + \sigma_z) - (\sigma_0 - \nu\sigma_0 - \nu q)\right] \\ \varepsilon^e_\theta &= \frac{1}{E}\left[\sigma_\theta - \nu(\sigma_r + \sigma_z) - (\sigma_0 - \nu\sigma_0 - \nu q)\right] \\ \varepsilon^e_z &= \frac{1}{E}\left[\sigma_z - \nu(\sigma_\theta + \sigma_r) - (q - 2\nu\sigma_0)\right].\end{aligned} \tag{21}$$

The stress equilibrium equation is given by

$$\frac{d\sigma_r}{d\rho} + \frac{\sigma_r - \sigma_\theta}{\rho} = 0. \tag{22}$$

The stress equilibrium differential equation for the $i$th annulus is expressed by

$$\frac{\sigma_{r(i)} - \sigma_{r(i-1)}}{\rho_{(i)} - \rho_{(i-1)}} + \frac{H\left(\overline{\sigma}_{\theta(i)}\right)}{\overline{\rho}_{(i)}} = 0, \tag{23}$$

where $H(\overline{\sigma}_{\theta(i)}) = \sigma_c(m_{(i-1)}\overline{\sigma}_{\theta(i)}/\sigma_c + s_{(i-1)})^{a_{(i-1)}}$, $\overline{\rho}_{(i)} = (\rho_{(i)} + \rho_{(i-1)})/2$, and $\overline{\sigma}_{(i)} = (\sigma_{(i)} + \sigma_{(i-1)})/2$.

The normalized inner radius $\rho_{(i)} = r_{(i)}/R$ can be expressed as

$$\rho_{(i)} = \rho_{(i-1)}\frac{2H\left(\overline{\sigma}_{\theta(i)}\right) - \Delta\sigma_r}{2H\left(\overline{\sigma}_{\theta(i)}\right) + \Delta\sigma_r}. \tag{24}$$

If the annuli are sufficiently thin in the case of axial symmetry, then the strain-displacement relationships can be described according to the model presented by Brown et al. [27] as

$$\frac{r_j}{r_{j-1}} = \frac{2\varepsilon_{\theta(j-1)} - \varepsilon_{r(j-1)} - \varepsilon_{r(j)}}{2\varepsilon_{\theta(j)} - \varepsilon_{r(j-1)} - \varepsilon_{r(j)}}. \quad (25)$$

The normalized inner radius is defined as follows:

$$\rho_{(j)} = \frac{r_{(j)}}{R}. \quad (26)$$

Then, (25) is simplified to

$$\frac{\rho_{(j)}}{\rho_{(j-1)}} = \frac{2\varepsilon_{\theta(j-1)} - \varepsilon_{r(j-1)} - \varepsilon_{r(j)}}{2\varepsilon_{\theta(j)} - \varepsilon_{r(j-1)} - \varepsilon_{r(j)}}. \quad (27)$$

The stain-displacement relationships can be given by

$$\begin{aligned} \varepsilon_r &= \frac{du}{dr} \\ \varepsilon_\theta &= \frac{u}{r}. \end{aligned} \quad (28)$$

The compatibility equation can be written in the general form as follows:

$$\frac{d\varepsilon_\theta}{dr} + \frac{\varepsilon_\theta - \varepsilon_r}{r} = 0. \quad (29)$$

Combining (26) and (29), the normalized compatibility equation can be expressed as follows:

$$\frac{d\varepsilon_\theta}{d\rho} + \frac{\varepsilon_\theta - \varepsilon_r}{\rho} = 0. \quad (30)$$

The total strain in plastic zone is the sum of the elastic and plastic strains as follows:

$$\begin{aligned} \varepsilon_\theta &= \varepsilon_\theta^p + \varepsilon_\theta^e \\ \varepsilon_r &= \varepsilon_r^p + \varepsilon_r^e \\ \varepsilon_z &= \varepsilon_z^p + \varepsilon_z^e. \end{aligned} \quad (31)$$

The following equations can be obtained by (30):

$$\begin{aligned} \frac{d\varepsilon_\theta^p}{d\rho} + \frac{\varepsilon_\theta^p - \varepsilon_r^p}{\rho} &= -\frac{d\varepsilon_\theta^e}{d\rho} - \frac{\varepsilon_\theta^e - \varepsilon_r^e}{\rho} \\ \varepsilon_\theta^e - \varepsilon_r^e &= \frac{1+\nu}{E}(\sigma_\theta - \sigma_r) \end{aligned} \quad (32)$$

$$\frac{d\varepsilon_\theta^p}{d\rho} + \frac{\varepsilon_\theta^p - \varepsilon_r^p}{\rho} = -\frac{d\varepsilon_\theta^e}{d\rho} + \frac{1+\nu}{E}\frac{H(\sigma_\theta)}{\rho}. \quad (33)$$

Combination of (32) and (33) leads to

$$\begin{aligned} &\Delta\varepsilon_{\theta(i)}^p \left( \frac{1}{\Delta\rho_{(i)}} + \frac{(k_3 - k_1)}{\overline{\rho}_{(i)} k_3} \right) \\ &= \frac{1+\nu}{E}\frac{H(\overline{\sigma}_{\theta(i)})}{\overline{\rho}_{(i)}} - \frac{\Delta\varepsilon_{\theta(i)}^e}{\Delta\rho_{(i)}} - \frac{1}{\overline{\rho}_{(i)}}\left(\varepsilon_{\theta(i-1)}^p - \varepsilon_{r(i-1)}^p\right), \end{aligned} \quad (34)$$

where $\Delta\rho_{(i)} = \rho_{(i)} - \rho_{(i-1)}$, $k_1 = (\sqrt{3}(2\sigma_1 - \sigma_2 - \sigma_3)/12\sqrt{J_2} - 1/3)n + (1/\sigma_c)(2\sigma_1 - \sigma_2 - \sigma_3)$, and $k_3 = (\sqrt{3}(2\sigma_3 - \sigma_2 - \sigma_1)/12\sqrt{J_2} - 1/3)n + (1/\sigma_c)(2\sigma_3 - \sigma_2 - \sigma_1)$.

The increments of the circumferential, radial, and axial strains can be, respectively, expressed by

$$\begin{aligned} \Delta\varepsilon_{\theta(i)}^p &= \frac{((1+\nu)/E)\left(H(\overline{\sigma}_{\theta(i)})/\overline{\rho}_{(i)}\right) - \Delta\varepsilon_{\theta(i)}^e/\Delta\rho_{(i)} - \left(1/\overline{\rho}_{(i)}\right)\left(\varepsilon_{\theta(i-1)}^p - \varepsilon_{r(i-1)}^p\right)}{\left(1/\Delta\rho_{(i)} + (k_3 - k_1)/\overline{\rho}_{(i)} k_3\right)} \\ \Delta\varepsilon_{r(i)}^p &= \Delta\varepsilon_{\theta(i)}^p \frac{k_1}{k_3} \\ \Delta\varepsilon_{z(i)}^p &= \Delta\varepsilon_{\theta(i)}^p \frac{k_2}{k_3}. \end{aligned} \quad (35)$$

Then, the total strain can be given by

$$\begin{aligned} \varepsilon_{\theta(i)} &= \varepsilon_{\theta(i-1)} + \Delta\varepsilon_{\theta(i)}^e + \Delta\varepsilon_{\theta(i)}^p \\ \varepsilon_{r(i)} &= \varepsilon_{r(i-1)} + \Delta\varepsilon_{r(i)}^e + \Delta\varepsilon_{r(i)}^p \\ \varepsilon_{z(i)} &= \varepsilon_{z(i-1)} + \Delta\varepsilon_{z(i)}^e + \Delta\varepsilon_{z(i)}^p. \end{aligned} \quad (36)$$

Therefore, we can obtain the plastic radius as follows:

$$R = \frac{r_0}{\rho_{(i)}} \quad (37)$$

The displacement at each ring can be obtained by

$$u = \varepsilon_{\theta(i)} R. \quad (38)$$

The displacement of the annulus at radius $r_j$ is expressed as

$$u_{(j)} = -\varepsilon_{\theta(j)} r_{(j)}. \quad (39)$$

The displacements of the annulus at radius ($r_j$) and plastic radius ($R$) are obtained through the numerical stepwise procedure in combination with MATLAB.

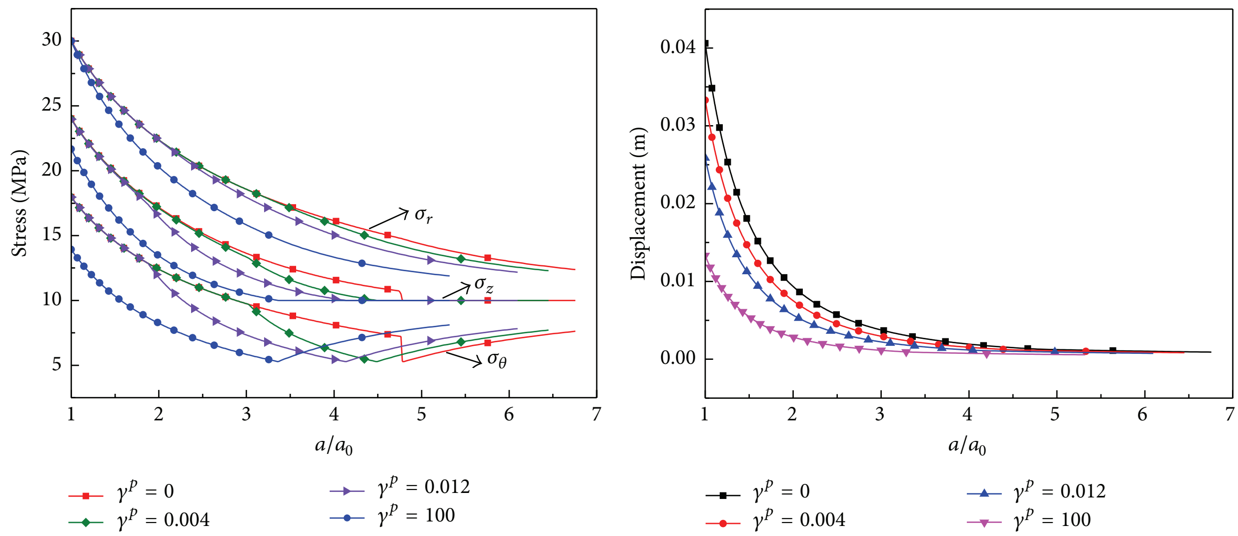


(a) Stresses

(b) Displacements

FIGURE 3: Displacement and stress with the different critical values of strain-softening parameters.

TABLE 1: Results by the proposed approach and Vesic's solution [1].

| $r_p/a_u$ | | 2 | 3 | 4 | 5 | 6 | 7 |
|---|---|---|---|---|---|---|---|
| $p$ (MPa) | Vesic | 21.9 | 27.6 | 32.4 | 36.6 | 40.4 | 43.9 |
| | H-B | 22.8 | 28.3 | 33.0 | 37.0 | 40.5 | 43.6 |
| Differences | — | 4.1% | 2.5% | 1.9% | 1.1% | 0.3% | 0.7% |

## 6. Validations

To confirm the validity and accuracy of the proposed approach based on the generalized H-B failure criterion, the results of the proposed approach are compared with those of Vesic's solution [1] for rock mass with the following data: $a_u = 0.25$ m, $\sigma_0 = 10$ MPa, $E = 5500$ MPa, $\nu = 0.25$, $a = 0.55$, $s = 0.0039$, $m = 1.7$, $\sigma_c = 10$ MPa, and $\psi = 0^\circ$ [28]. However, Vesic's result [1] for rock mass is based on the M-C failure criteria. In order to compare the result of the proposed solution, the technique of the equivalent M-C and generalized H-B strength parameters is adopted [29]. The strength parameters for the M-C failure criterion are as follows: $c = 1.36591$ MPa, $\varphi = 18.8549$ MPa.

As seen from Table 1, the expansion pressures of the proposed approach based on the generalized H-B failure criterion agree well with those of Vesic's solution [1]. In the comparison, the maxim differences of expansion pressure $p$ do not exceed 5% for the cylindrical expansion cavity. The validations show that the numerical stepwise method is effective in analyzing the cavity expansion problem.

## 7. Numerical Analysis and Discussions

The stress and displacement of cylindrical cavity with out-of-plane stress considered are calculated to emphasize the influences of the out-of-plane stress. In order to study the effect of strain-softening, dilation parameter, strength parameter, elastic modulus, and Poisson's ratio with the out-of-plane stress considered, several examples are performed in the proposed solution.

The input data of the proposed solution based on the generalized H-B failure criterion presented by Sharan [28] are as follows: $\sigma_0 = 10$ MPa, $E = 5500$ MPa, $\nu = 0.25$, $p_{\rm in} = 30$ MPa, $r_0 = 0.25$ m, $\sigma_c = 10$ MPa, $q = 10$ MPa, $m_p = 1.7$, $s_p = 0.0039$, $a_p = 0.55$, $m_r = 0.8$, $s_r = 0.0019$, $a_r = 0.5$.

*7.1. Effects of the Strain-Softening Parameters.* Softening parameters are important characteristic of strain-softening surrounding rock. Its value can be acquired from two methods. One is determined by the plastic shear strain $\gamma^p = \varepsilon_1^p - \varepsilon_3^p$, and the other is to use the principal strain to determine $\varepsilon_1^p$. In order to analyze the influence of softening parameters, four cases are analyzed using the proposed approach (i.e., Case 1: $\gamma^p = 0$; Case 2: $\gamma^p = 0.004$; Case 3: $\gamma^p = 0.012$; Case 4: $\gamma^p = 100$). The results are shown in Figure 3.

Figure 3 illustrates that the values of stress and displacement decrease with the softening parameter ($\gamma^p$) increasing. It can be seen from Figure 3 that the displacements of the proposed approach would be reduced significantly if $\gamma^p$ increases from 0 to 100. For example, displacement is 0.041 m, 0.033 m, and 0.013 m when $\gamma^p$ equals 0, 0.004, and 100, respectively. The reduction of the displacement is 28% if $\gamma^p$ increases from 0 to 0.004.

*7.2. Effect of Dilation Parameters.* In order to examine the effects of dilation parameters that consider out-of-plane stress, four cases are performed using the proposed approach (i.e., Case 1: $n = 0.1$; Case 2: $n = 1$; Case 3: $n = 2$; Case 4: $n = 4$). The results are shown in Figures 4 and 5.

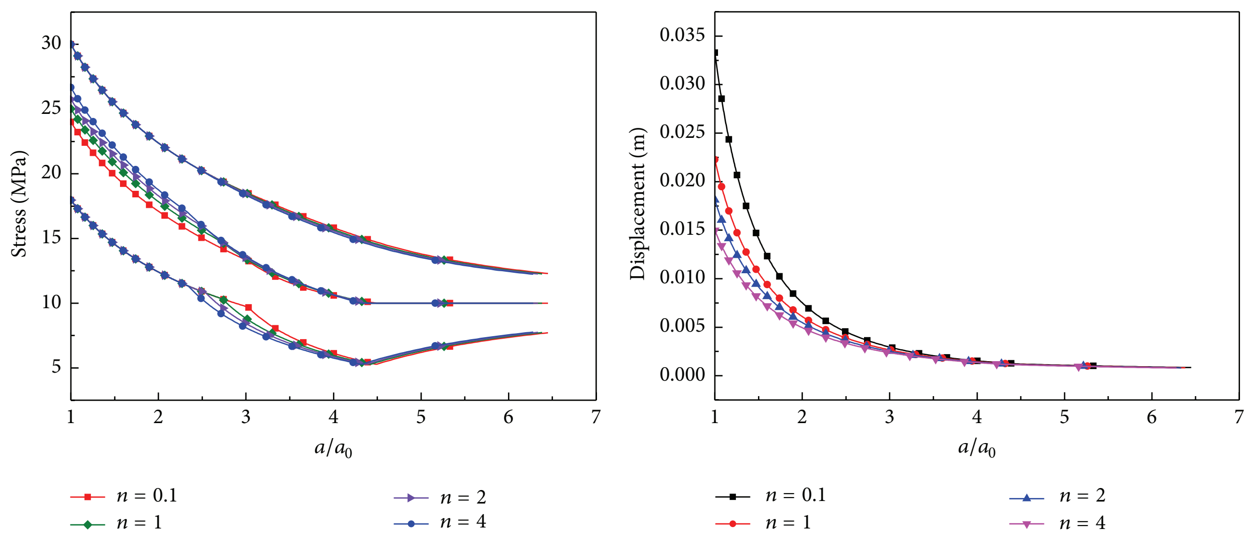


(a) Stresses

(b) Displacements

FIGURE 4: Displacement and stress with the different dilation parameters.

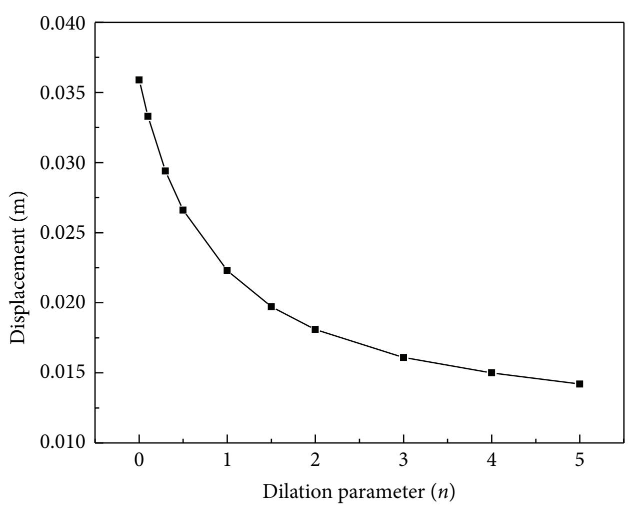


FIGURE 5: Displacements with the different dilation parameters.

The effects of dilation parameters on the displacement and stress considering out-of-plane stress are significant. As shown in Figure 4, displacements of this study decreases from 0.033 m to 0.015 m with dilation parameters increasing from 0.1 to 4 and it reduces by $\Delta = (0.033 - 0.015)/0.033 \times 100\% = 54.5\%$. Therefore, the effects of dilation parameters should be taken into account carefully.

Figure 5 demonstrates the relationship between the displacements of cavity and the dilation parameter. The displacements decrease continuously with the increasing of the dilation parameter. However, when the dilation parameter is greater than 3.0, the displacements decrease slightly. But the displacements decrease significantly when the dilation parameter ranges from 0 to 3.0. Therefore, the effect of dilation parameter changes with different dilation parameter.

*7.3. Effects of Strength Parameters.* In order to detect the effect of strength parameter ($m$) on stress and displacement, three different cases are analyzed using the proposed approach. They are Case 1: $m_p = m_r = 0.8$; Case 2: $m_p = 1.7$, $m_r = 0.8$; Case 3: $m_p = m_r = 1.7$. The results are shown in Figure 6.

It is shown from Figure 6 that the effect of strength parameter on stress and displacement is significant, and all of them decrease with strength parameter increasing. Moreover, the plastic radius as shown in Figure 6(a) is 1.423 m and 0.853 m when $m_p$ and $m_r$ equal 0.8 and 1.7, respectively. It can be seen from Figure 6(b) that the displacement decreases from 0.050 m to 0.014 m with strength parameters increasing from 0.8 to 1.7. Thus, the effects of strength parameter on stress and displacement are significant.

*7.4. Effects of Elasticity Modulus.* To identify the effect of modulus of elasticity on the stress and displacement, three different cases are analyzed using the proposed method. They are Case 1: $E_p = E_r = 3500$; Case 2: $E_p = 5500$, $E_r = 3500$; Case 3: $E_p = E_r = 5500$. The results are depicted in Figure 7.

The effect of the elastic modulus on the displacement that considers out-of-plane stress is significant, while the influence of the elastic modulus on stress is insignificant. As shown in Figure 7, the displacement decreases from 0.056 m to 0.014 m as the elastic modulus increases from 3500 MPa to 5500 MPa. However, the stresses for three different cases are relatively steady. Therefore, the effects of elastic modulus on displacement should be taken into consideration.

*7.5. Effects of Poisson Ratio.* To determine the effects of Poisson's ratio on stress and displacement, the results are shown in Figure 8, for three different cases of Poisson's ratio using the proposed approach: Case 1: $\nu_p = \nu_r = 0.25$; Case 2: $\nu_p = 0.35$, $\nu_r = 0.25$; Case 3: $\nu_p = \nu_r = 0.35$.

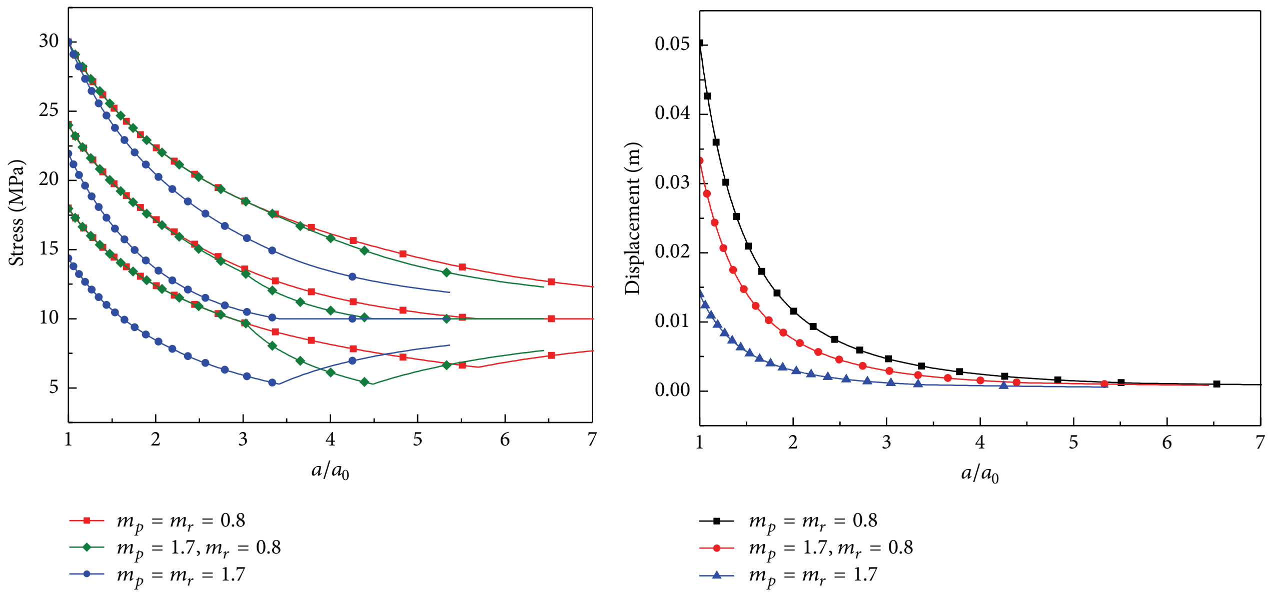


(a) Stresses

(b) Displacements

Figure 6: Displacement and stress with the different strength parameters $m$.

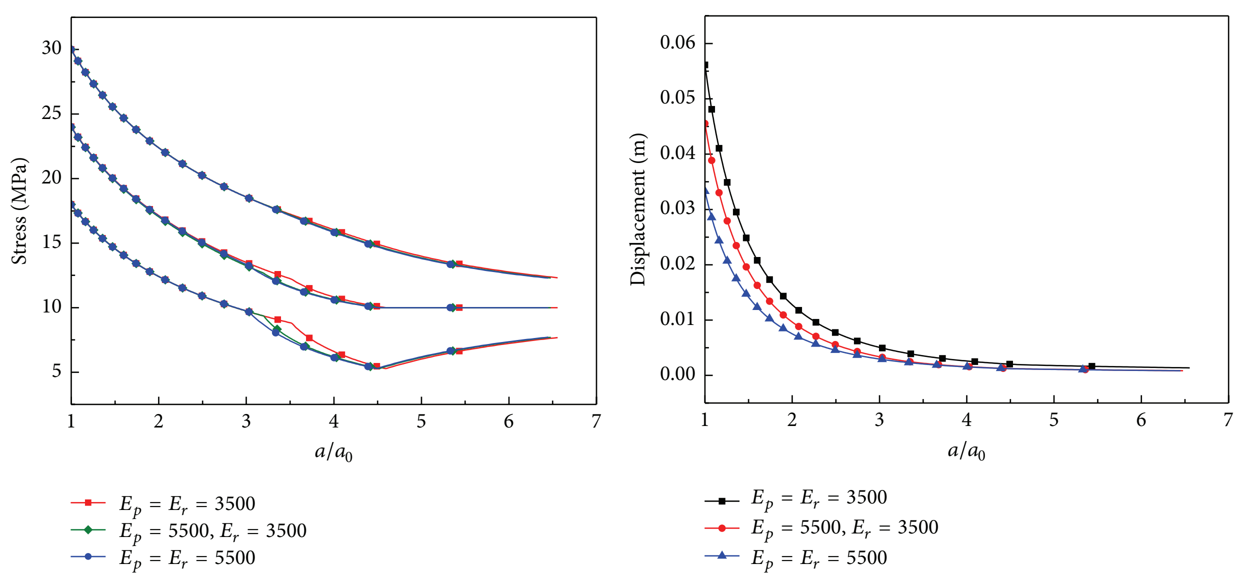


(a) Stresses

(b) Displacements

Figure 7: Displacement and stress with the different elastic modulus.

Apparently, it can be seen from Figure 8 that variations of different curves are very small. Hence, Poisson's ratio has little effect on the stress and displacement. For example, displacements vary from 0.033 m to 0.031 m, and plastic radius varies from 1.122 m to 1.118 m as $v$ increase from 0.25 to 0.35.

## 8. Conclusions

Solutions of stress, displacement, and plastic radius for cylindrical cavity expansion were proposed by considering out-of-plane stress and the quasi-plane strain-softening problem based on the generalized Hoek-Brown failure criterion. The intermediate principal stress is obtained by 3D plastic potential function and Hooke's law, which is deformation-dependent. The validity and accuracy of the proposed solution are confirmed by Vesic's solution [1]. Furthermore, the effects of strain-softening, dilation parameter, strength parameter, elastic modulus, and Poisson's ratio on stresses and displacement of cavity expansion are studied with the new approach.

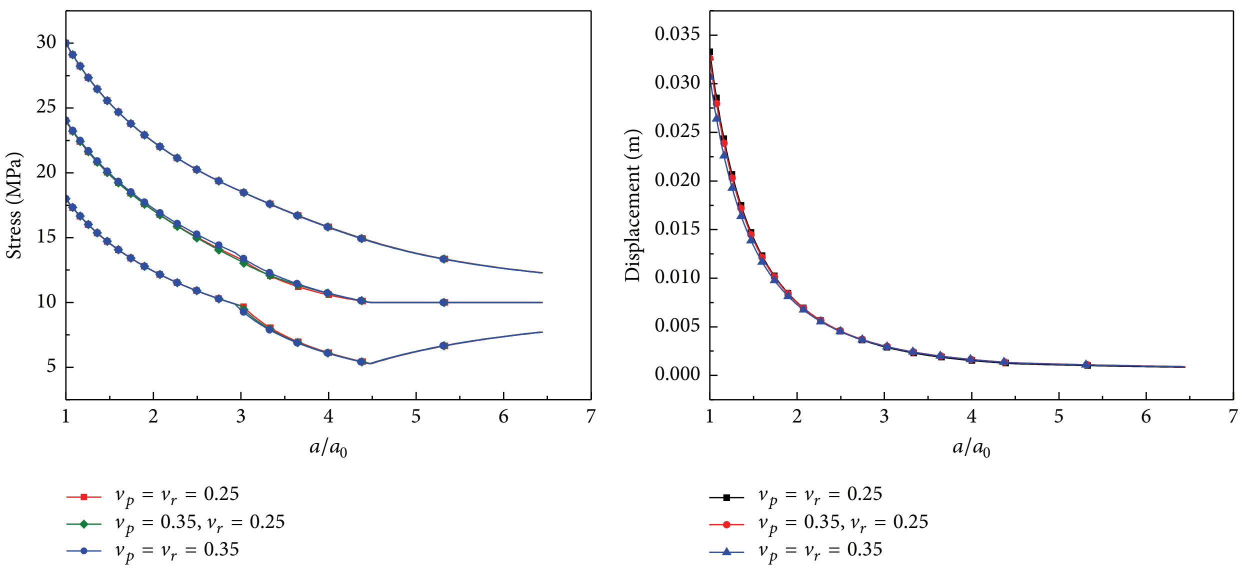


(a) Stresses

(b) Displacements

FIGURE 8: Displacement and stress with the different Poisson's ratio.

## Competing Interests

The authors declare that they have no competing interests.

## References


[1] A. S. Vesic, "Expansion of cavities in infinite soil mass," *Journal of Geotechnical Engineering*, vol. 98, no. 3, pp. 265–290, 1972.

[2] J. P. Carter, J. R. Booker, and S. K. Yeung, "Cavity expansion in cohesive frictional soils," *Géotechnique*, vol. 36, no. 3, pp. 349–358, 1986.

[3] D. Durban and P. Papanastasiou, "Cylindrical cavity expansion and contraction in pressure sensitive geomaterials," *Acta Mechanica*, vol. 122, no. 1–4, pp. 99–122, 1997.

[4] D. Durban, "Large strain solution for pressurized elasto/plastic tubes," *Journal of Applied Mechanics*, vol. 46, no. 1, pp. 228–230, 1979.

[5] D. Durban and M. Kubi, "General solution for the pressurized elastoplastic tube," *Journal of Applied Mechanics*, vol. 59, no. 1, pp. 20–26, 1992.

[6] D. Durban, "Finite straining of pressurized compressible elasto-plastic tubes," *International Journal of Engineering Science*, vol. 26, no. 9, pp. 939–950, 1988.

[7] I. F. Collins and H. S. Yu, "Undrained cavity expansions in critical state soils," *International Journal for Numerical and Analytical Methods in Geomechanics*, vol. 20, no. 7, pp. 489–516, 1996.

[8] X.-D. Pan and E. T. Brown, "Influence of axial stress and dilatancy on rock tunnel stabblity," *Journal of Geotechnical Engineering*, vol. 122, no. 2, pp. 139–146, 1996.

[9] L. F. Cao, C. I. Teh, and M. F. Chang, "Undrained cavity expansion in modified Cam clay I: theoretical analysis," *Géotechnique*, vol. 51, no. 4, pp. 323–334, 2001.

[10] E. Alonso, L. R. Alejano, F. Varas, G. Fdez-Mańin, and C. Carranza-Torres, "Ground response curves for rock masses exhibiting strain-softening behaviour," *International Journal for Numerical and Analytical Methods in Geomechanics*, vol. 27, no. 13, pp. 1153–1185, 2003.

[11] Y.-K. Lee and S. Pietruszczak, "A new numerical procedure for elasto-plastic analysis of a circular opening excavated in a strain-softening rock mass," *Tunnelling and Underground Space Technology*, vol. 23, no. 5, pp. 588–599, 2008.

[12] K.-H. Park, B. Tontavanich, and J.-G. Lee, "A simple procedure for ground response curve of circular tunnel in elastic-strain softening rock masses," *Tunnelling and Underground Space Technology*, vol. 23, no. 2, pp. 151–159, 2008.

[13] X. L. Yang and J. F. Zou, "Cavity expansion analysis with non-linear failure criterion," *Geotechnical Engineering*, vol. 164, no. 1, pp. 41–49, 2011.

[14] S. L. Chen and Y. N. Abousleiman, "Exact drained solution for cylindrical cavity expansion in modified cam clay soil," *Géotechnique*, vol. 63, no. 6, pp. 510–517, 2013.

[15] S. L. Chen and Y. N. Abousleiman, "Exact undrained elasto-plastic solution for cylindrical cavity expansion in modified cam clay soil," *Géotechnique*, vol. 62, no. 5, pp. 447–456, 2012.

[16] S. L. Wang, S. D. Yin, and Z. J. Wu, "Strain-softening analysis of a spherical cavity," *International Journal for Numerical and Analytical Methods in Geomechanics*, vol. 36, no. 2, pp. 182–202, 2012.

[17] H. Zhou, H. Liu, and G. Kong, "Influence of shear stress on cylindrical cavity expansion in undrained elastic-perfectly plastic soil," *Geotechnique Letters*, vol. 4, pp. 203–210, 2014.

[18] H. Zhou, H. Liu, G. Kong, and Z. Cao, "Analytical solution for pressure-controlled elliptical cavity expansion in elastic-perfectly plastic soil," *Géotechnique Letters*, vol. 4, no. 2, pp. 72–78, 2014.

[19] H. Zhou, H. L. Liu, G. Q. Kong, and X. Huang, "Analytical solution of undrained cylindrical cavity expansion in saturated soil under anisotropic initial stress," *Computers and Geotechnics*, vol. 55, pp. 232–239, 2014.

[20] A.-Z. Lu, G.-S. Xu, F. Sun, and W.-Q. Sun, "Elasto-plastic analysis of a circular tunnel including the effect of the axial in

situ stress," *International Journal of Rock Mechanics and Mining Sciences*, vol. 47, no. 1, pp. 50–59, 2010.

[21] J. F. Zou and Z. He, "Numerical approach for strain-softening rock with axial stress," *Proceedings of the Institution of Civil Engineers—Geotechnical Engineering*, vol. 169, no. 3, pp. 276–290, 2016.

[22] Z. Jin-Feng and S. Yu, "Theoretical solutions of a circular tunnel with the influence of the out-of-plane stress based on the generalized Hoek-Brown failure criterion," *International Journal of Geomechanics*, vol. 16, no. 3, Article ID 06015006, 2016.

[23] J. F. Zou and S. Q. Zuo, "An approximate solution for the cylindrical cavity expansion under the non-axisymmetric displacement boundary condition on hypotenuse," *International Journal of Geotechnical Engineering*, 2016.

[24] J. F. Zou and Z. Q. Xia, "Solutions for displacement and stress in strain-softening surrounding rock incorporating the effects of hydraulic-mechanical coupling and rockbolt effectiveness," *Geotechnical and Geological Engineering*, 2016.

[25] J. F. Zou and S. S. Li, "Theoretical solution for displacement and stress in strain-softening surrounding rock under hydraulic-mechanical coupling," *Science China Technological Sciences*, vol. 58, no. 8, pp. 1401–1413, 2015.

[26] J. F. Zou, W. Q. Tong, and J. Zhao, "Energy dissipation of cavity expansion based on generalized non-linear failure criterion under high stresses," *Journal of Central South University*, vol. 19, no. 5, pp. 1419–1424, 2012.

[27] E. T. Brown, J. W. Bray, B. Ladanyi, and E. Hoek, "Ground response curves for rock tunnels," *Journal of Geotechnical Engineering*, vol. 109, no. 1, pp. 15–39, 1983.

[28] S. K. Sharan, "Exact and approximate solutions for displacements around circular openings in elastic-brittle-plastic Hoek-Brown rock," *International Journal of Rock Mechanics & Mining Sciences*, vol. 42, no. 4, pp. 542–549, 2005.

[29] X.-L. Yang and J.-H. Yin, "Slope equivalent Mohr-Coulomb strength parameters for rock masses satisfying the Hoek-Brown criterion," *Rock Mechanics and Rock Engineering*, vol. 43, no. 4, pp. 505–511, 2010.